

A Method for Estimating the Lung Clinical Target Volume DVH from IMRT with and without Respiratory Gating

J. H. Kung^a, P. Zygmanski^b, N. Choi^a, G. T. Y. Chen^a

^a: Department of Radiation Oncology, Massachusetts General Hospital and Harvard Medical School, Boston, MA
^b: Department of Radiation Oncology, Brigham and Women's Hospital and Harvard Medical School, Boston, MA

ABSTRACT

Motion of lung tumors from respiration has been reported in the literature to be as large as of 1-2 cm. This motion requires an additional margin between the Clinical Target Volume (CTV) and the Planning Target Volume (PTV). While such a margin is necessary, it may not be sufficient to ensure proper delivery of Intensity Modulated Radiotherapy (IMRT) to the CTV during the simultaneous movement of the DMLC. Gated treatment has been proposed to improve normal tissues sparing as well as to ensure accurate dose coverage of the tumor volume. The following questions have not been addressed in the literature: a) what is the dose error to a target volume without gated IMRT treatment? b) what is an acceptable gating window for such treatment. In this study, we address these questions by proposing a novel technique for calculating the 3D dose error that would result if a lung IMRT plan were delivered without gating. The method is also generalized for gated treatment with an arbitrary triggering window. IMRT plans for three patients with lung tumor were studied. The treatment plans were generated with HELIOS for delivery with 6 MV on a CL2100 Varian linear accelerator with a 26 pair MLC. A CTV to PTV margin of 1 cm was used. An IMRT planning system searches for an optimized fluence map $\Phi(x, y)$ for each port, which is then converted into a dynamic MLC file (DMLC). The DMLC file contains information about MLC subfield shapes and the fractional Monitor Units (MUs) to be delivered for each subfield. With a lung tumor, a CTV that executes a quasi periodic motion $z(t)$ does not receive $\Phi(x, y)$, but rather an Effective Incident Fluence $EIF(x, y)$. We numerically evaluate the $EIF(x, y)$ from a given DMLC file by a coordinate transformation to the Target's Eye View (TEV). In the TEV coordinate system, the CTV itself is stationary, and the MLC is seen to execute a motion $-z(t)$ that is superimposed on the DMLC motion. The resulting $EIF(x, y)$ is inputted back into the dose calculation engine to estimate the 3D dose to a moving CTV. In this study, we model respiratory motion as a sinusoidal function with an amplitude of 10 mm in the superior-inferior direction, a period of 5 seconds, and an initial phase of zero.

The table below summarizes the impact of motion on the volume of CTV treated to the prescription dose with and without motion.

Patient	no motion		1cm motion	
	Vol(Rx)	3D(max)/D(Rx)	Vol(Rx)	3D(max)/D(Rx)
1	95%	103%	92%	107%
2	68%	105%	50%	105%
3	95%	105%	90%	105%

Key Words: organ motion, intensity modulated, dose error

1. INTRODUCTION

In 3D Conformal Radiation Treatment (3DCRT), a Clinical Target Volume (CTV) to Planning Target Volume (PTV) margin is added to accommodate for beam delivery error, patient setup error, and organ motion. Yu¹ and Chui² have shown that in IMRT treatment of lung cancer, a CTV-PTV margin is necessary but not sufficient. In the extreme case, a Synchronous Motion (SM) between the Dynamic Multi Leaf Collimator (DMLC) and periodic respiratory motion can result in as much as +/- 100% fluence errors to portions of the tumor volume (Fig. 1).

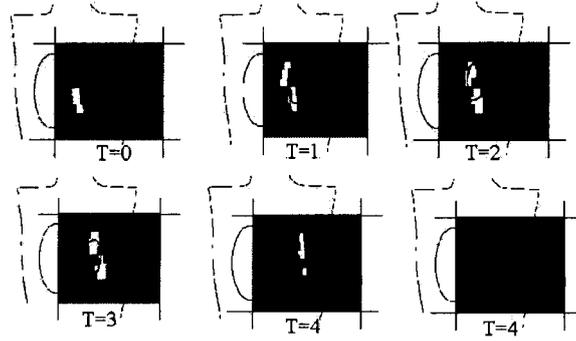


Fig.1. Dose prescription, dose per fraction, and number of ports for each of the IMRT plans.

For this reason, Stein et al.,³ and Jiang⁴ have argued in favor of compensator based IMRT. A proposed alternative is gated treatment for lung IMRT. Shimizu⁵ et al have demonstrated the importance of gated CT scanning for lung cancer treatment with 3DCRT. In gated teletherapy⁶⁻¹⁰, radiation from a linear accelerator is triggered only when a target volume is within a fixed window about its mean position. In the literature, the following questions have not been addressed for gated IMRT treatment: (a) If gating is not applied during IMRT to a moving target, what is the effect of Synchronous Motion on the DVH of the CTV? (b) for gated treatment, what is an acceptable triggering window? (c) how can one create a leaf motion sequence that is least sensitive to the SM effect? In this study, we address (a) and (b) by proposing a novel technique for calculating the 3D dose error resulting from an IMRT plan that is delivered without gating. The method is then generalized to calculate the dose when gated treatment with an arbitrary triggering window is applied. The results are specific to a given patient's anatomy and IMRT plan.

2. METHODS AND MATERIALS

A. Conceptual Foundation

The HELIOSTM IMRT system (Varian Medical Systems, Palo Alto, CA) was used in this study. In IMRT planning, one chooses the photon energy, radiation portals (e.g., number of fields and their orientations), and specifies a prescription. The prescription is in the form of a desired dose volume histogram (DVH) for a given target and organs at risk. The planning system then calculates an optimized fluence map $\Phi_{opt}(x,y)$ for each portal. Each $\Phi_{opt}(x,y)$ is subsequently converted into a leaf sequence file, or DMLC file. The DMLC file contains data on each MLC subfield, including its shape and the fractional Monitor Units (MUs) to be delivered with each subfield. The superposition of each MLC subfield aperture weighted by its corresponding MU yields the composite physical fluence $\Phi_{phy}(x,y)$. In general, there can be a small difference between $\Phi_{phy}(x,y)$ and $\Phi_{opt}(x,y)$ because the latter fluence was calculated without taking into consideration any physical limitation of an MLC. In this work, we neglect these differences and use $\Phi(x,y)$ to denote either fluence^{11,12}. Consider a Clinical Tumor Volume (CTV) in the lung that moves periodically along the longitudinal axis during irradiation, described by $z(t)$. To simplify, we assume that the CTV moves as a rigid body (no rotation). Future work will address a more generalized case where rotation may be present. From the Target's Eye View (TEV), the target itself is stationary and the MLC executes a trajectory seen as $-z(t)$ superimposed on the conventional DMLC leaf motion (Figure 2). Therefore in the Target's Eye View, the function $-z(t)$ characterizes a beam delivery error as a function of time. The target volume does not receive the optimized $\Phi(x,y)$ but rather an $EIF(x,y)$ because of the $z(t)$ motion. While the planning system dose calculations are based on $\Phi(x,y)$, we propose that an effective dose to the moving target should be recalculated using the $EIF(x,y)$. Dose to nonmoving normal tissues should continue to be calculated with

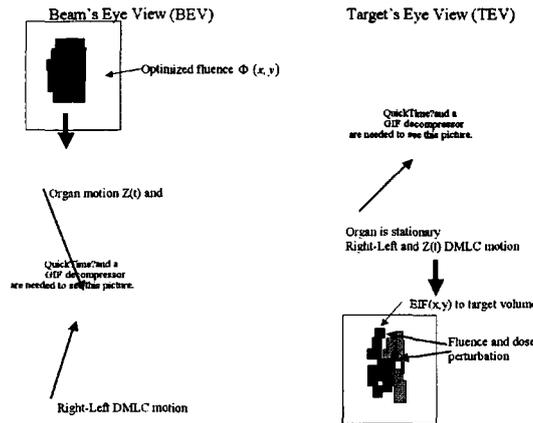


Fig 2. From the beam's eye view, the MLC leaf movement is characterized by right / left motion and organ movement is described by the function $z(t)$. In the Target's Eye View (TEV), the tumor itself is stationary and a motion of $-z(t)$ is superimposed on

$\Phi(x,y)$. The effective fluence $EIF(x,y)$ can be analytically calculated from a given DMLC file by projecting each subfield aperture weighted with its corresponding MU onto a calculational grid that incorporates the periodic motion $z(t)$ (Fig. 2). The $EIF(x,y)$ can then be reintroduced into the dose calculation engine of the planning system to recalculate the 4D dose to the CTV (Fig. 3). In the calculation of the $EIF(x,y)$ for gated treatment with an irradiation window (w), $z(t)$ is truncated for an amplitude greater than (w) as shown in Fig. 4. Several qualifying statements and assumptions should be made: a) in the dose calculation with $EIF(x,y)$, we assume that the radiological depth to the tumor volume does not change with organ motion¹³. We are primarily interested in identifying the fluence and subsequent dose error from Synchronous Motion between the DMLC and organ motion, which previously other investigators have stated can be as large as 100%. With a typical attenuation of 3% per cm of tissue for a 6MV beam, neglecting a possible change in depth is justified. b)

The CTV to PTV margin is a function of daily setup error, linac delivery error, and organ motion. We consider the case where the daily setup and linac delivery errors are zero. This permits the primary focus of the analysis to be on the dosimetric consequences of organ motion due to respiration. c) In principle, the calculation of $EIF(x,y)$ from a DMLC file requires detailed knowledge of the phase of organ motion at the time linac beam is turned on. In the present analysis, for IMRT delivery with multiple DMLC ports, we assume that each beam is turned on at an instant the tumor volume is at its mean position, or specifically at a phase of zero. Zyganski¹⁴ et al have shown that the DMLC to $EIF(x,y)$ calculation with typical clinical parameters is only mildly dependent on the initial phase of respiration (e.g, 2Gy/f, 300MU/min, respiratory amplitude of +/-1cm, respiratory period of 5 seconds). d) We confine the discussion to IMRT delivery on a Varian linear accelerator since the experiments were performed on vendor specific equipment.

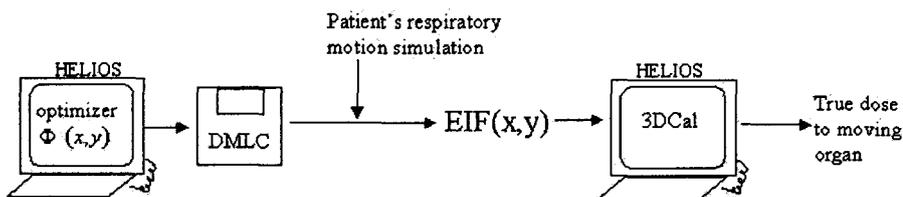


Fig 3. A block diagram outlining how organ motion is incorporated into the effective incident fluence $EIF(x,y)$ and how the HELIOS dose engine is used to calculate a cumulative 4D dose to a moving target volume.

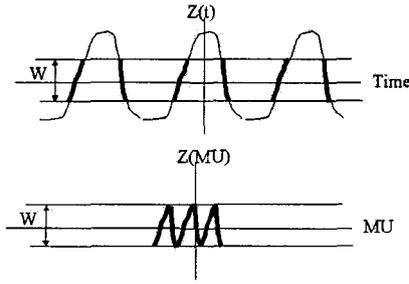


Fig 4. A schematic of organ motion, $z(t)$, as function of beam ON time (t). For gating triggered within window (w), the radiation beam is turned ON only when $|z(t)| < w$.

B. DMLC to Fluence Map Conversion:

The method developed requires the ability to calculate a fluence matrix $\Phi(x, y)$ / $EIF(x, y)$ from a DMLC file; $\Phi(x, y)$ / $EIF(x, y)$ is then used to calculate the 3D dose distribution using a dose calculation engine of an IMRT treatment planning system. This process is tested here by the methods described. Fig. 5 schematically shows the DMLC test file that was used

The leaf pair opening is 1cm at 100 cm SAD, and the central 10 leaf pairs of the 26 pair MLC are used. The resulting irradiation is a region of approximately uniform film density 10 cm to 12 cm along the X jaw and 10 cm along Y jaw. We will refer to this DMLC file irradiation as the 1 cm Average Leaf Pair Opening (ALPO) irradiation¹⁴. From this DMLC file, we calculated $\Phi(x, y)$ for a jaw opening of $14 \times 14 \text{ cm}^2$ with MU = 200. A fluence matrix resolution is chosen to be 2.5 mm x 2.5 mm. For regions inside the static jaw openings but under the tungsten MLC leaves, a leaf transmission factor of $T=1.5\%$ is used. The DMLC to $\Phi(x, y)$ conversion is written in Mathematica v3.0. The effective fluence $\Phi(x, y)$ is re-inputted into HELIOS and the 3D dose calculation is performed for a rectangular geometrical phantom. For a detail explanation of how $\Phi(x, y)$ is determined from a DMLC file, see reference Kung¹². We compare the dose value at $d = 5 \text{ cm}$ along central axis as determined by three different methods: a) dose calculated by HELIOS. b) Hand calculation of dose using the Clarkson method and c) experimental measurement using film.

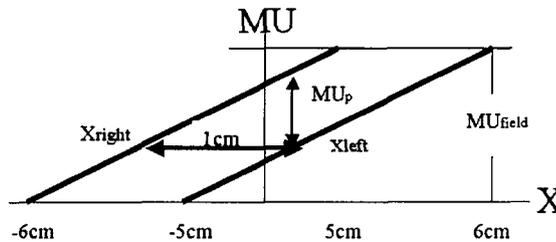


Fig 5. Leaf trajectory for the 1cm ALPO DMLC test. Each of the inner 10 leaves undergo an identical trajectory.

C. Validating the $EIF(x, y)$ Calculation

We next tested the process of incorporating organ motion when converting from DMLC files to $EIF(x, y)$. This study was done with the 1 cm ALPO DMLC irradiation (Fig. 5) with assumed motion of $Z(t) = A \sin(2\pi / T + \theta)$. For this study, parameters were $A=1\text{cm}$, $T=10 \text{ seconds}$, $\theta = 0$. The DMLC tolerance was set at 2 mm. With the linac dose rate of 600MU/min, the effective dose rate was up to 50% slower. Therefore we used 400 MU/min to convert from leaf position as function of cumulative Monitor Units (MU) to leaf position as function of beam ON time. The resulting $EIF(x, y)$ was re-inputted into HELIOS and 3D dose distribution was calculated for a flat geometrical phantom. A motorized table (Fig. 6) was constructed; it moves on rails with a near periodic sinusoidal motion in one dimension¹⁵, e.g., $Z(t) = A \sin(2\pi / T + \theta)$, $A=1\text{cm}$, $T=10 \text{ seconds}$, $\theta = 0$. A verification film was placed at $d = 5 \text{ cm}$ in a solid

water phantom and irradiated with the 1 cm ALPO DMLC configuration. The optical density of a film was converted to dose with a measured H&D calibration curve.

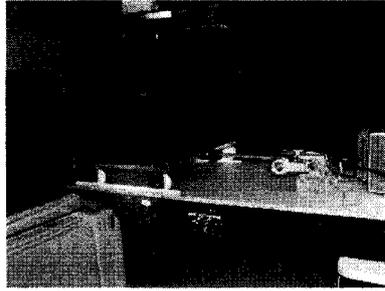


Fig 6. Motorized table used to simulated dose delivered to a moving organ

Finally, we compared the penumbra at a depth of 5 cm in the coronal plane as calculated by HELIOS with the penumbra as measured on film.

D. Patient Specific Treatment Plans

Scans from three lung patients involved in an IMRT concomitant boost protocol were selected. Planning CT scans with slice thickness of 3.75 mm were acquired on a helical CT scanner. The CT scans were ungated, and in this study we assumed the tumor volume as acquired represented the true mean position and shape of the tumor volume. CTV's were drawn on axial CT scans by a radiation oncologist. A CTV to PTV margin of 1 cm was applied. In this study we assumed no daily setup error; therefore the 1 cm margin was for the respiratory motion. IMRT plans were first generated with HELIOS system. Table I lists the number of fields and prescription used for each plan. Fig. 7(a,b) show the 3D volumes for the Patient 1. An IMRT plan output consisted of MU, DMLC, gantry angle, collimator angle, couch angle, and jaws for each IMRT port. Effective Incident Fluences $EIF(x, y)$'s were calculated from each plan output. $EIF(x, y)$ for each port was put back into HELIOS dose calculation engine to calculate a 4D dose to the CTV that would result if an IMRT plan were delivered without gating. In the calculation of $EIF(x, y)$ for each patient specific DMLC file, respiratory motion is modeled as before by a sinusoidal function with an amplitude of 10 mm in the superior-inferior direction, a period of 5 seconds, and a phase of zero.

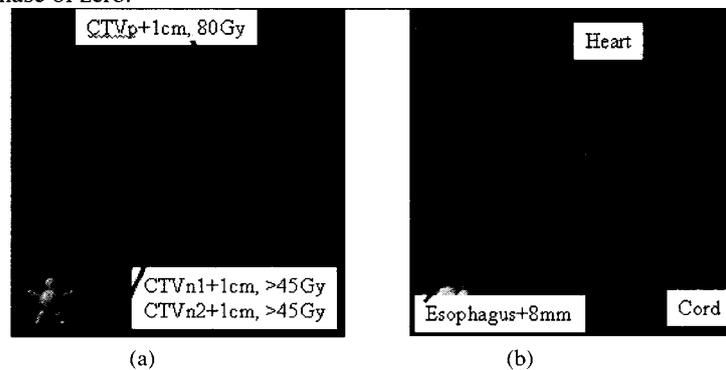


Fig 7(a, b). 3D views of primary target volume and two nodal volumes for the IMRT plan for patient 1.

We assume no motion in the other principal axes. The $EIF(x, y)$ is computed as before with a $2.5 \times 2.5 \text{ mm}^2$ resolution to match the calculation grid used in Helios. The IMRT plans were computed for a dose rate of 300 MU/min (5 MU/sec). The Varian MLC hardware verifies leaf position every 50 milliseconds. With a DMLC tolerance setting of 2 mm, an effective dose rate for these IMRT plans were on average 4 MU/sec. This latter value was used to convert leaf positions as function of MU to leaf positions as function of time.

3. RESULTS

A. DMLC File to Dose Calculation

Table II shows comparison of dose at $d = 5 \text{ cm}$ for the 1 cm ALPO DMLC irradiation. The difference between HELIOS and independent hand Clarkson calculation is 1.1%; the difference between the film measured dose and hand calculation

was 2%. This confirms our ability to use the HELIOS system to calculate a 3D dose distribution starting from an arbitrary DMLC file. A brief explanation of the hand calculation of dose for the 1cm ALPO irradiation is in order. In Fig. 5, MU_{field} is the total number of Monitor Units (MU) for the port. MU_p and MU_T denotes the primary (under open leaves) and MLC transmitted fluences, respectively. From the figure, $MU_p = (1cm/11cm)MU_{field}$. Because of a Radiation Field Offset (RFO) ^{11,14,16,17} of 0.75 mm for a Varian MLC with 6MV, the effective radiation aperture is larger than the corresponding light fields by 0.75 mm per rounded leaf end. Therefore,

$$MU_p = [(1cm + 2RFO) / 11cm] MU_{field} = (1.15cm / 11cm) MU_{field} \quad (1)$$

And $MU_T = (MU_{field} - MU_p)T$, where $T=1.5\%$ is MLC transmission factor. The sum of primary and transmission fluence is $MU_{\Sigma} \equiv MU_p + MU_T = 0.118MU_{field}$. In this hand calculation, we neglect tongue and groove effects and interleaf transmission¹⁸. Because the resulting fluence is approximately $10 \times 10 \text{ cm}^2$ uniform, dose $D(d, jaw)$ at a depth (d) and a jaw opening (jaw) can be readily calculated.

$$D(d, jaw) = (1cGY / MU) \cdot S_c(jaw) \cdot S_p(aperture) \cdot TPR(d, aperture) \cdot MU_{\Sigma} \quad (2)$$

Standard notation convention for S_c, S_p, TPR is used; these variables are: collimator scatter factor, phantom scatter factor, and tissue phantom ratios, respectively.

B. Validating the DMLC to $EIF(x, y)$ calculation

Fig. 8 shows a verification film placed at $d = 5 \text{ cm}$ and irradiated with the 1 cm ALPO DMLC file. The film and solid water phantom was placed on top of the motorized table. As a comparison, Fig. 9 displays the coronal isodose line as calculated by HELIOS system using $EIF(x, y)$. We define $P(80/20)$ as the largest width between the 80% and 20% isodose lines. Table III shows a comparison of $P(80/20)$ and $P(80/30)$ penumbra widths as calculated by HELIOS and as measured with film. Agreement is within 1 mm. The result confirms our ability to incorporate motion into $EIF(x, y)$ and to calculate 3D dose distribution starting from a DMLC file.

C. Patient Studies

Fig. 10 shows an axial isodose and field configuration for the IMRT plan for Patient 1. Figs. 11 (a,b,c) show the $DVH(CTV)$ calculated with and without organ motion. For Patient 1 (Fig. 11a), the DVH for the primary site with respiration has a softer shoulder at 96% to 106% dose level. The 45 Gy prescription to lymph nodes corresponds to the 59% isodose line; therefore, the differences in DVH's between motion and no motion at 75% to 95% dose levels may not be clinically significant. In the plan for Patient 2 (Fig. 11b), the IMRT plan provides only limited coverage of the GTV because of its proximity to the spinal cord. For this patient, the difference in the $DVH(CTV)$ with respiration motion was 98% to 103%. Table IV summarizes the motion / no motion comparison results. We define $Vol(Rx)$ as the volume covered the 96% to 108% dose level. In the analysis of Patient 3 (Fig. 11c), the $DVH(CTV)$ with motion had a softer shoulder in by the specified prescription isodose line

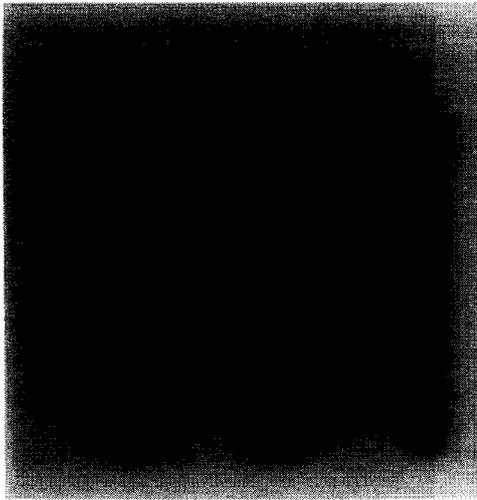


Fig 8. A verification film irradiated at $d = 5$ cm, 6MV with the 1 cm ALPO DMLC. The film was irradiated on a moving table.

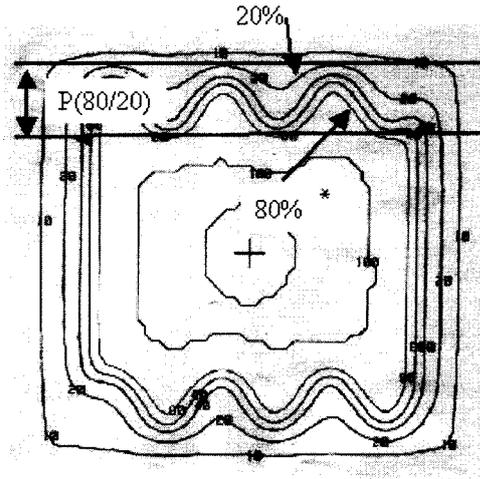


Fig 9. EIF(x,y) for the 1cm ALPO DMLC is re-inputted into HELIOS dose engine. This is the coronal isodose distribution at $d = 5$ cm as calculated by HELIOS. P(80/20) is the largest distance between the 80% and the 20% isodose lines.



Fig 10. IMRT field arrangement and the axial isodose lines for Patient 1. Nodal volume 2 is not visible on this specific slice.

DVH of GTV and nodes for patient 1 (A=1cm, T=5 seconds)

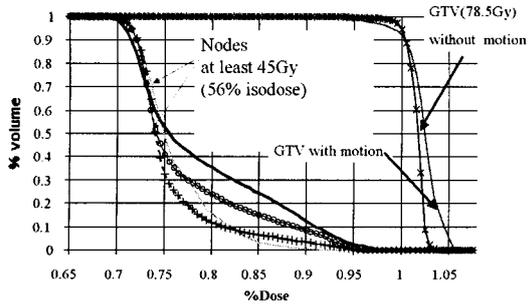


Fig. 11.a

DVH of GTV and node for patient 3 (A=1cm, T=5 seconds)

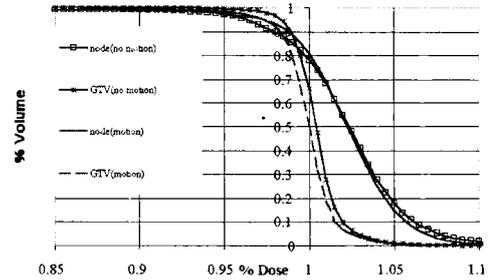


Fig.11.b

DVH of GTV for patient 2 (A=1cm, T=5 seconds)

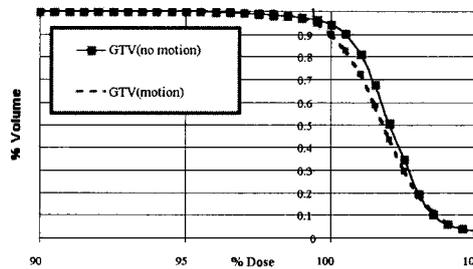


Fig.11. c

Figs 11(a,b,c). Comparison of DVH's including motion and neglecting motions.

4. CONCLUSION AND DISCUSSION

We described a technique to estimate the 3D dose error to a moving tumor resulting from IMRT treatment without gating. For gated treatments with gating window (w), the method can be used to determine whether a residual organ motion with an amplitude (w) results in an acceptable dose error to CTV. The method is fundamentally general; however, results specifically depend on a given patient's anatomy, the details of the respiration induced motion, and the specific DMLC file generated in the inverse planning process. Consider a patient being treated with N static fields in which linac beam ON time for each port is much longer than periodicity of a CTV motion. Then an organ motion can result in under dosing only to a surface of the CTV. With an appropriate CTV to PTV margin this under dosing to a CTV surface is removed. In IMRT, CTV to PTV margin is still necessary to ensure coverage of CTV boundary under organ motion; the change in DVH(CTV) can only be from Synchronous Motion (SM) effect, which can result in either under dosing and/or over dosing to the interior of CTV. We conclude that for patient 1 and patient 3 IMRT plans, the dose error to the CTV from SM effect is small and just as in the static field case CTV to PTV margin was adequate. For these two plans, a need for gated treatment with gating window (w) can be decided solely by the need to improve the normal tissues sparing. For patient 2 IMRT plan, the CTV coverage that changed from 68% to 50% can not necessarily be attributed to the SM effect alone. This is because in the IMRT plan for patient 2 CTV was in the vicinity of a spinal cord (i.e., CTV motion was confined to PTV but PTV was not covered by prescription isodose). For this patient, gated treatment and gating level (w) should be chosen to reduce CTV to PTV margin (i.e., spare dose to spinal cord) and to ensure dose error to CTV from an organ motion is clinically acceptable. Future work we will address a dosimetric verification in phantoms, with more realistic organ motion parametrization, dependence on phase¹⁴ and linac dose rate¹⁹.